

Journal of Organometallic Chemistry, 427 (1992) 9–21

Elsevier Sequoia S.A., Lausanne

JOM 22372

Structure and dynamics of hindered organosilicon compounds. The conformations of symmetrical $(\text{Me}_3\text{Si})_3\text{C}$ and $(\text{PhMe}_2\text{Si})_3\text{C}$ derivatives

Anthony G. Avent

School of Chemistry and Molecular Sciences, University of Sussex, Brighton BN1 9QJ (UK)

Simon G. Bott¹

Inorganic Chemistry Laboratory, University of Oxford, Oxford OX1 3QB (UK)

John A. Ladd, Paul D. Lickiss

Department of Chemistry and Applied Chemistry, University of Salford, Salford M5 4WT (UK)

and Alan Pidcock

Department of Chemistry, Lancashire Polytechnic, Preston PR1 2TQ (UK)

(Received September 16, 1991)

Abstract

At low temperatures the methyl region of the ^1H and ^{13}C NMR spectra of $(\text{Me}_3\text{Si})_3\text{CSiCl}_3$ and the ^1H NMR spectrum of $(\text{Me}_3\text{Si})_3\text{CSiBr}_3$ each show three signals of equal intensity and the ^{29}Si NMR spectrum of the trichloride shows only one Me_3Si signal. These data are consistent with the methyls within each Me_3Si group becoming inequivalent. Compounds containing the $(\text{PhMe}_2\text{Si})_3\text{C}$ group are able to adopt different conformations at low temperature; in $(\text{PhMe}_2\text{Si})_3\text{CSiCl}_3$ the phenyl groups mesh together while in $(\text{PhMe}_2\text{Si})_3\text{CBr}$ they are separated by methyl groups. These different arrangements of the ligand can readily be distinguished by ^1H NMR spectroscopy, and the conformation in the case of $(\text{PhMe}_2\text{Si})_3\text{CSiCl}_3$ has been confirmed in the solid state by X-ray crystallography.

Introduction

In recent years Eaborn and co-workers have prepared a large number of organometallic compounds containing either the bulky $(\text{Me}_3\text{Si})_3\text{C}$ ("trisyl") or the $(\text{PhMe}_2\text{Si})_3\text{C}$ group, which have often been shown to have unusual structures or

Correspondence to: Dr. P.D. Lickiss, Department of Chemistry and Applied Chemistry, University of Salford, Salford M5 4WT, UK.

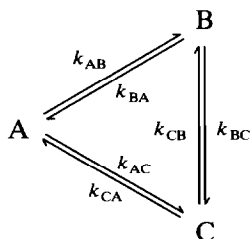
¹ Present address: Department of Chemistry, The University of North Texas, Denton, TX 76203-5068, USA.

exhibit novel reactivity [1]. The presence of these bulky groups in silicon compounds allows restricted rotation about the central C–Si bonds to be observed by NMR spectroscopy at readily accessible temperatures. This has already been investigated for the related compounds $(\text{Me}_3\text{Si})_2\text{C}(\text{SiMe}_2\text{ONO}_2)(\text{SiPh}_2\text{Me})$ and $(\text{Me}_3\text{Si})_2\text{C}(\text{SiMe}_2\text{OMe})(\text{SiPh}_2\text{Cl})$ which at -90°C show ^1H NMR spectra in which all the methyl groups are distinguishable [2,3]. The spectra of the methoxy silane revealed the existence of two enantiotopomeric forms of these molecules whose rate and mechanism of interconversion could be conveniently monitored using the coalescence of pairs of signals in both the ^{13}C and the ^{29}Si NMR spectra and from 2D NMR spectra.

The present study was undertaken to examine more symmetrical compounds containing either the $(\text{Me}_3\text{Si})_3\text{C}$ or the $(\text{PhMe}_2\text{Si})_3\text{C}$ group to ascertain the nature of the processes averaging methyl and phenyl sites in the molecules and the preferred conformations of the ligands. For the trisyl group, where three-site chemical exchange is observed, internal rotation averages the methyl groups and this can be monitored by both ^1H and ^{13}C NMR spectroscopy.

In order to gain further insight into the dynamics of the processes involved, a complete line-shape analysis was required. McConnell [4] has shown how the familiar Bloch equations of NMR can be modified to take account of the chemical exchange between different sites by the inclusion of terms representing the rates at which magnetization is lost and regained by the individual sites.

For a 3-site exchange system



the equations take the form, for site A,

$$\dot{u}_A + u_A/T_{2A} + (\omega - \omega_A)v_A = -(k_{AB} + k_{AC})u_A + k_{BA}u_B + k_{CA}u_C$$

$$\dot{v}_A + v_A/T_{2A} - (\omega - \omega_A)u_A + \omega_1 M_z^A = -(k_{AB} + k_{AC})v_A + k_{BA}v_B + k_{CA}v_C$$

$$\dot{M}_z^A + (M_z^A - M_0^A)/T_{1A} - \omega_1 v_A = -(k_{AB} + k_{AC})M_z^A + k_{BA}M_z^B + k_{CA}M_z^C$$

and similarly for sites B and C.

Under equilibrium conditions, the time-dependent terms \dot{u}_A , \dot{v}_A , and \dot{M}_z^A are zero. The nine equations then become a complete set of ordinary simultaneous linear equations. If it is assumed that there is no r.f. saturation, *i.e.* ω_1 is very small, then $M_z \approx M_0$ for each site and the number of equations is reduced to six. We have written a FORTRAN77 computer program to solve these equations (in matrix form) using the NAG [5] routine F04ATF which employs Crout's factorization method [6].

It is merely $v = v_A + v_B + v_C$ that is required, since this corresponds to the absorption mode in which the high resolution NMR spectrum is displayed. The line-shapes so generated are then compared with those observed.

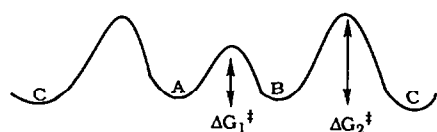
Results and discussion

The ^1H and ^{13}C NMR spectra of $(\text{Me}_3\text{Si})_3\text{CSiCl}_3$ and the ^1H NMR spectrum of $(\text{Me}_3\text{Si})_3\text{CSiBr}_3$ all show the presence of three chemically distinct types of methyl groups at temperatures below 200 K, the resonances for which coalesce and become indistinguishable at temperatures above 250 K. In contrast, the ^{29}Si NMR spectra over the same temperature range show a single Me_3Si resonance. The internal motions must, therefore, involve interchange of the methyl positions only.

The line-shape changes observed in the ^1H and ^{13}C NMR spectra between 200 and 250 K could not be described by one activation energy (which would require all the rate constants to be equal and to have a temperature dependence given by the Eyring equation:

$$k = \frac{\kappa k_{\text{B}} T}{h} \exp\left(\frac{-\Delta G^\ddagger}{RT}\right)$$

where x is the transmission coefficient, k_{B} is Boltzmann's constant and the other symbols have their usual meanings), so there must be at least two processes involved. Because of the internal symmetry of the rotating groups one can therefore picture the potential profile to be:



so that the rate constants $k_{\text{AB}} = k_{\text{BA}}$ are controlled by the free energy of activation ΔG_1^\ddagger (and lead to the first coalescence) while all the remaining rate constants are equal and are controlled by ΔG_2^\ddagger . The strategy adopted was therefore to compute line-shapes (based on initial estimates of ΔG_1^\ddagger and ΔG_2^\ddagger) covering the whole temperature range investigated and to visually compare them with the corresponding observed line-shapes. The initial values of ΔG_1^\ddagger and ΔG_2^\ddagger were then refined

Table 1

Free energies of activation for internal rotation in Me_3Si and Me_3C derivatives

	ΔG_1^\ddagger (kJ mol ⁻¹)	ΔG_2^\ddagger (kJ mol ⁻¹)	Ref.
$(\text{Me}_3\text{Si})_3\text{CSiCl}_3$	44.0 ± 0.5	48.5 ± 0.5	This work
$(\text{Me}_3\text{Si})_3\text{CSiBr}_3$	45.0 ± 0.5	52.5 ± 0.5	This work
$(\text{Me}_3\text{C})_3\text{SiH}$	21.3	28.4	7 ^a
	- ^b	25.5 ± 1.3	7 ^c
$(\text{Me}_3\text{C})_3\text{SiCl}$	- ^b	37.7	8 ^d
	- ^b	31.7 ± 3	9 ^d
$(\text{Me}_3\text{C})_3\text{SiBr}$	- ^b	39.6	8 ^d
	- ^b	32.7 ± 3	9 ^d
$(\text{Me}_3\text{C})_3\text{SiI}$	- ^b	40.8	8 ^d
	- ^b	43.2 ± 3	9 ^d
$(\text{Me}_3\text{C})_3\text{SiMe}$	25.1	38.5	10 ^a
	- ^b	33.0 ± 1.3	11 ^d
$[(\text{Me}_3\text{C})_3\text{PMe}]^+ \text{I}^-$	26.3 ± 3.3	39.7 ± 2.1	12 ^c

^a Empirical force field calculation. ^b Not observed in NMR spectrum. ^c Calculated by line-shape analysis of ^{13}C NMR spectra. ^d Calculated by line-shape analysis of ^1H NMR spectra.

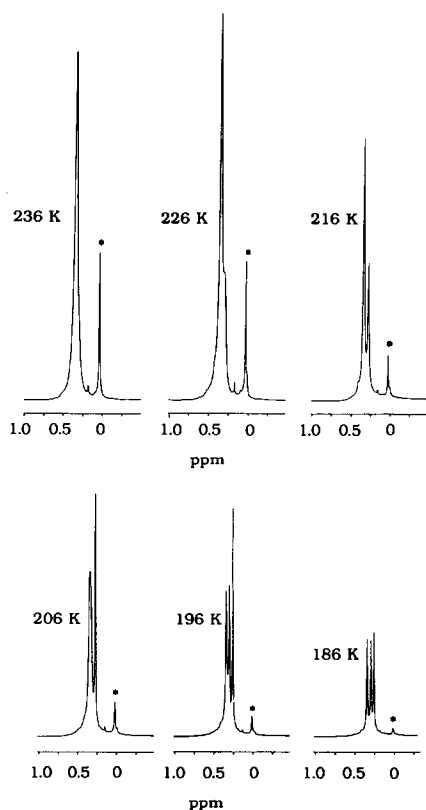


Fig. 1. Variable temperature ^1H NMR spectra of $(\text{Me}_3\text{Si})_3\text{CSiCl}_3$. Spectra were recorded on CDCl_3 solutions at 360 MHz. The corresponding ^{13}C NMR spectra of $(\text{Me}_3\text{Si})_3\text{CSiCl}_3$ show the two signals at low field to be those averaged by the low energy process. The ^1H spectra of $(\text{Me}_3\text{Si})_3\text{CSiBr}_3$ and the ^{13}C spectra of $(\text{Me}_3\text{Si})_3\text{CSi}(\text{OH})_3$ [38] both show that the two signals at high field are averaged by the low energy process. The signal marked by an asterisk is due to an impurity.

to give the best visual fit. The results given in Table 1 represent the best fit for both the ^1H and ^{13}C NMR spectra in each case. For comparison, Table 1 also gives values of free energy barriers in species structurally related to trisilyl compounds.

Mislow [7] has reported evidence, based on empirical force field calculations and dynamic NMR studies, that the rotation of the *tert*-butyl groups in $^1\text{Bu}_3\text{SiH}$ is a correlated motion. He described different torsional pathways denoted sss or ess depending on whether the rotation proceeded via an eclipsed (e) or a staggered (s) conformation. His force field calculations showed that the ess pathway had the higher barrier (28.4 kJ mol^{-1}) and that it led to decoalescence of the methyl ^{13}C resonance into two signals with an intensity ratio 2:1 at 133 K. The lower energy sss pathway (21.3 kJ mol^{-1}) could not be observed down to 116 K.

The above analysis may be extended to the trisilyl compounds studied here. In a completely analogous fashion we observed an initial decoalescence of the methyl resonance in $(\text{Me}_3\text{Si})_3\text{CSiCl}_3$ (in both the ^1H , see Fig. 1, and ^{13}C NMR spectra) and in $(\text{Me}_3\text{Si})_3\text{CSiBr}_3$ (only the ^1H NMR spectra were recorded, for chemical shift data see Experimental section) into two signals with an intensity ratio 2:1

which was followed at a lower temperature by a further decoalescence of the more intense signal to give a total of three separate signals with an intensity ratio 1 : 1 : 1. We may therefore identify ΔG_2^\ddagger with the *ess* pathway and ΔG_1^\ddagger with the *sss* pathway. The considerable increase in the numerical values of these barriers to internal rotation over those found in ${}^t\text{Bu}_3\text{SiH}$ and the other compounds given in Table 1 is attributable to the extra bulk of the SiX_3 group. The presence of a fourth bulky group around the central atom thus makes trisilyl silicon derivatives particularly amenable to study by variable temperature NMR spectroscopy.

An electron diffraction study of $(\text{Me}_3\text{Si})_3\text{CSiCl}_3$ has revealed [13] that the SiX_3 "umbrella" has been forced to close from the tetrahedral X-Si-X angle of 109.4° to 103.9° owing to the size of the three Me_3Si groups present, and there must be a concomitant effect on the barriers to rotation of the trimethylsilyl groups. It was also found [13] that the four SiX_3 groups attached to the central carbon in $(\text{Me}_3\text{Si})_3\text{CSiCl}_3$ were twisted away from a fully staggered conformation by about 23° to relieve the steric strain caused by non-bonded interactions. Such twisting away from the ideal T_d to T symmetry has also been found in gas-phase electron diffraction studies of $(\text{Me}_3\text{Si})_3\text{CPH}_2$ [14], $(\text{Me}_3\text{Si})_4\text{C}$ [15], and $(\text{Me}_3\text{Si})_4\text{Si}$ [16]. Empirical force field calculations on $(\text{Me}_3\text{C})_4\text{M}$ ($\text{M} = \text{C}, \text{Si}$ or Ge) and $(\text{Me}_3\text{Si})_4\text{M}$ ($\text{M} = \text{C}$ or Si) have indicated similar conformations [17]. The effects of the twisting, which leads to chiral molecules, on NMR spectra has been discussed previously [3,7,12] and the packing of chiral $(\text{Me}_3\text{Si})_3\text{C}$ groups in crystal lattices has also been investigated [18]. The ${}^1\text{H}$ variable temperature NMR spectra and the X-ray crystal structure of $[(\text{Me}_3\text{Si})_3\text{CSiCl}_2]_2\text{O}$ have also been reported [19]. (For a discussion of previous attempts to observe the three expected methyl resonances in $(\text{Me}_3\text{C})_3\text{MX}$ species by low temperature NMR spectroscopy see ref. 12.)

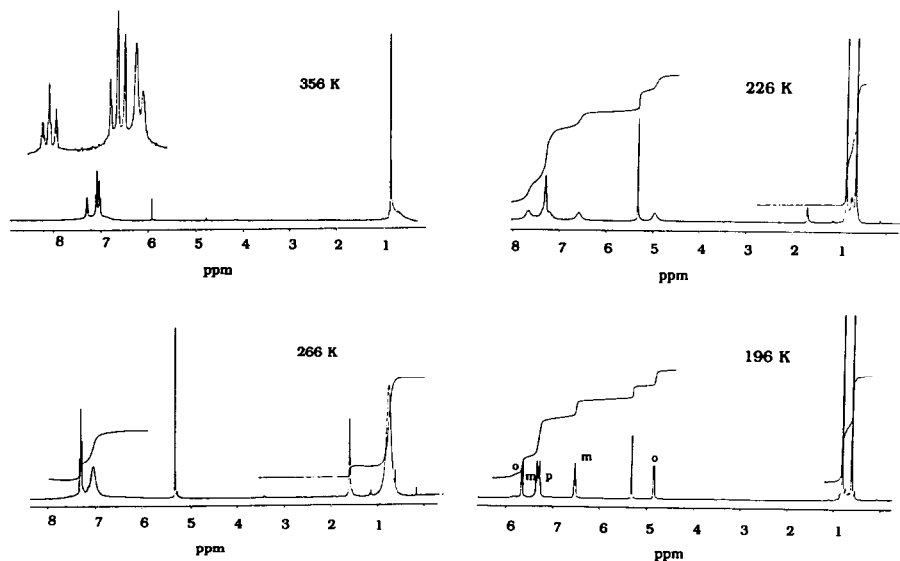


Fig. 2. Variable temperature ${}^1\text{H}$ NMR spectra of $(\text{PhMe}_2\text{Si})_3\text{CSiCl}_3$. The spectrum recorded at 356 K was of a $\text{Cl}_2\text{C}=\text{CCl}_2/\text{Cl}_2\text{HCCHCl}_2$ solution and the others were of a CD_2Cl_2 solution. The sharp signals at approximately 5.9 and 5.3 ppm are due to solvent and the signal at 1.6 ppm is due to water. In the 196 K spectrum *o*, *m*, and *p* denote *ortho*, *meta*, and *para* proton signals.

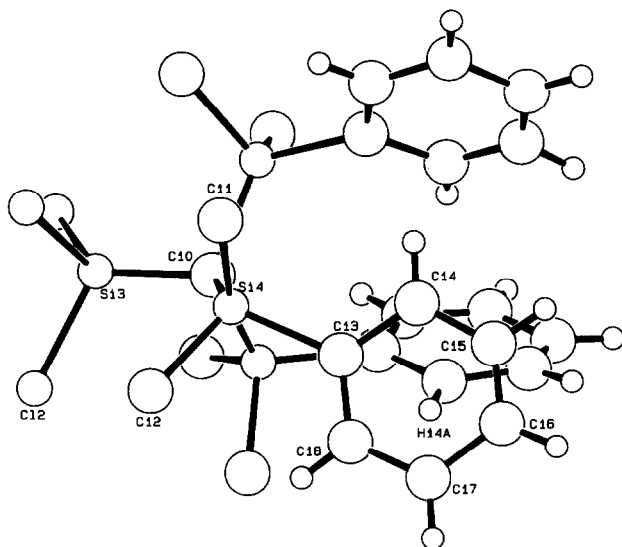


Fig. 3. The molecular structure of $(\text{PhMe}_2\text{Si})_3\text{CSiCl}_3$ together with the atom numbering for molecule 2 in the unit cell (see Discussion and Tables 2 and 3). The methyl hydrogen atoms are omitted for clarity.

The ^1H NMR spectrum of $(\text{PhMe}_2\text{Si})_3\text{CSiCl}_3$ (Fig. 2) shows temperature-dependent features associated with the resonances of the phenyl protons and with those of the methyl groups. At 193 K the inequivalent *ortho* protons of the phenyl ring show a large internal chemical shift difference of 2.80 ppm (1008 Hz). Coalescence of these signals occurs at 244 K which corresponds to a free energy barrier of 43.7 kJ mol $^{-1}$. The large chemical shift difference must derive from the proximity of one *ortho* proton to the face of an adjacent phenyl ring. At 193 K the methyl proton signals are separated by 0.196 ppm (70.5 Hz); coalescence occurs at 263 K corresponding to a free energy barrier of 53.1 kJ mol $^{-1}$. (In the ^{13}C spectrum the methyl signals are separated by 0.722 ppm (65.4 Hz) at 216 K and coalescence occurs at 266 ± 5 K which corresponds to a barrier of 53.8 ± 1 kJ mol $^{-1}$, in excellent agreement with value found from the proton spectrum.) It seems reasonable to conclude that the latter higher barrier corresponds to the *ess* pathway discussed earlier. The lower barrier has a magnitude which appears to correspond to the *sss* pathway of concerted rotations but it is not clear whether this process leads to an averaging of the *ortho* protons. An alternative explanation is that there is restricted rotation of the phenyl groups about their own Si–Ph bonds.

An X-ray crystallographic study of $(\text{PhMe}_2\text{Si})_3\text{CSiCl}_3$ was carried out in order to discover whether the conformation of the $(\text{PhMe}_2\text{Si})_3\text{C}$ group in the solid state might be similar to that in solution at low temperature. The molecular structure so derived, together with the atom numbering scheme, is shown in Fig. 3. The most important feature of the structure seen in the figure is the position of H14A above the aromatic ring C13–C18. A hydrogen atom near an aromatic ring experiences the ring current caused by the π -electrons; in the plane of the ring this causes a downfield chemical shift but above the ring the reverse occurs and an upfield shift is observed. This would, then, explain the low temperature ^1H NMR spectrum,

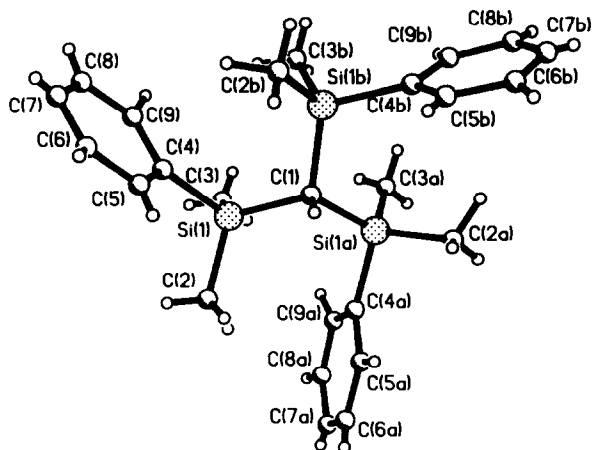


Fig. 4. The molecular structure of $(\text{PhMe}_2\text{Si})_3\text{CH}$. Redrawn using data from ref. 14.

one *ortho* proton from each ring being in a “normal” unperturbed environment and the other being situated above a phenyl ring and experiencing a strong upfield shift due to the ring current. This clearly suggests that the conformation of the $(\text{PhMe}_2\text{Si})_3\text{C}$ group is very similar at low temperature in solution to that in the solid state.

The ^1H NMR spectra of $(\text{PhMe}_2\text{Si})_3\text{CBr}$ at various temperatures show a different behaviour; at low temperature (173 K) the aromatic part of the spectrum is broad and in the same region as at room temperature. In the methyl region the signal decoalesces into two resonances at low temperature, one of which is shifted upfield to -0.725 ppm. The shift difference between the two signals is 1.26 ppm (454 Hz) and they coalesce at 216 ± 10 K which corresponds to a free energy barrier of 39.8 ± 2 kJ mol $^{-1}$. This is lower than the value calculated above in $(\text{PhMe}_2\text{Si})_3\text{CSiCl}_3$, presumably as a result of the smaller bulk of Br compared with SiCl_3 . Using the ring current argument applied above, it appears that in this case the conformation of the ligand is such that the phenyl rings do not interact with each other but that the methyl groups are constrained to be above an aromatic ring.

Although we have not determined the solid state structure of $(\text{PhMe}_2\text{Si})_3\text{CBr}$, Fig. 4 shows the structure of $(\text{PhMe}_2\text{Si})_3\text{CH}$ [20] in which the proposed structure, with phenyl rings widely separated and methyl groups centred on C(2), C(2a) and C(2b) are positioned above the aromatic rings defined by C(4a)–C(9a), C(4b)–C(9b) and C(4)–C(9), respectively. This fits well with the observed NMR spectra found for the monobromide. It would thus seem that the $(\text{PhMe}_2\text{Si})_3\text{C}$ group can adopt two different conformations in symmetrical compounds, one (as seen for the trichloride) in which the phenyl groups are folded away from the fourth substituent on the central carbon and are meshed together and another (as seen in the monobromide) in which the phenyl groups are spread apart and lie closer to the fourth substituent. The difference in conformation may be attributed to the size of the group R in symmetrical $(\text{PhMe}_2\text{Si})_3\text{CR}$ compounds; a large group such as SiCl_3 forces the phenyl groups together and a small group such as H or Br allows the phenyl groups to spread away from each other.

A variety of conformations, including those discussed above, of the $(\text{PhMe}_2\text{Si})_3\text{C}$ group have been found in other compounds by X-ray crystallography. In both the alkylgallium compound $[\text{Li}(\text{thf})_2(\mu\text{-Cl})_2\text{GaCl}\{\text{C}(\text{SiMe}_2\text{Ph})_3\}] \cdot \text{thf}$ [21] and in the cadmium compound $[\{\text{Cd}[\text{C}(\text{SiMe}_2\text{Ph})_3]\text{Br}(\text{H}_2\text{O})\}_2] \cdot \text{thf}$ [22] the phenyl groups are meshed together in a manner similar to that in $(\text{PhMe}_2\text{Si})_3\text{CSiCl}_3$, while in $(\text{PhMe}_2\text{Si})_3\text{CBF}(\text{OH})$ [23] and $[(\text{thf})_3\text{Li}(\mu\text{-H})_3\text{BC}(\text{SiMe}_2\text{Ph})_3]$ [24] the $(\text{PhMe}_2\text{Si})_3\text{C}$ groups are spread apart in a conformation similar to that found in $(\text{PhMe}_2\text{Si})_3\text{CH}$. In other compounds such as $(\text{PhMe}_2\text{Si})_3\text{CSnMe}_2\text{F}$ [25], $(\text{PhMe}_2\text{Si})_3\text{CPCl}_2$ [26], $(\text{PhMe}_2\text{Si})_3\text{CSiMe}_2\text{N}=\text{N}=\text{C}(\text{Me})-\text{N}=\text{N}$ [27], $[(\text{PhMe}_2\text{Si})_3\text{CCdBr}]_2$ [22], and $[(\text{PhMe}_2\text{Si})_3\text{CZnOH}]_2$ [28] the phenyl groups are arranged unsymmetrically such that one projects forwards, towards the fourth substituent, and the others are folded back, separated by methyl groups as in $(\text{PhMe}_2\text{Si})_3\text{CH}$.

The rather poor quality of data obtained in the X-ray crystallographic determination of $(\text{PhMe}_2\text{Si})_3\text{CSiCl}_3$ precludes detailed discussion of the structure, but several general points can be made. The Si-C bonds to the central carbon (average 1.96 Å) appear to be longer than the $\text{H}_3\text{C}-\text{Si}$ distances (average 1.85 Å), the Si-C-Si angles within the $(\text{PhMe}_2\text{Si})_3\text{C}$ group (average 112.6°) are larger than the $\text{Cl}_3\text{Si}-\text{C}-\text{Si}$ angles (average 106.1°) and the $\text{H}_3\text{C}-\text{Si}-\text{CH}_3$ angles (average 103.0°) are smaller than the $\text{C}_{\text{central}}-\text{Si}-\text{CH}_3$ angles (average 114.4°). The lengthening of the bonds to the central carbon compared to those around the periphery of the molecule and the closing up of the Me-Si-Me angles is also seen in the related compounds $(\text{PhMe}_2\text{Si})_3\text{CPCl}_2$ [26], $(\text{PhMe}_2\text{Si})_3\text{CSiMe}_2\text{N}=\text{N}=\text{C}(\text{Me})-\text{N}=\text{N}$ [27], $(\text{PhMe}_2\text{Si})_3\text{CSiMe}(\text{OH})$ [29] and $(\text{PhMe}_2\text{Si})_3\text{CSiMe}_2\text{OH}$ [30], but the $\text{Cl}_3\text{Si}-\text{C}-\text{Si}$ angles cannot be compared with the corresponding angles in these compounds owing to their lack of symmetry. A similar lengthening of bonds to the central carbon and the closing up of the Me-Si-Me angles to accommodate steric strain has also been found in $(\text{Me}_3\text{Si})_3\text{C}$ derivatives (see, for example, refs. 25 and 31).

Experimental

The samples of $(\text{Me}_3\text{Si})_3\text{CSiCl}_3$ and $(\text{PhMe}_2\text{Si})_3\text{CBr}$ were prepared as described previously [32,33].

Determination of the ^1H , ^{13}C and ^{29}Si NMR spectra

The NMR spectra were recorded using a Bruker WM360 instrument operating at 360 (^1H), 71.5 (^{29}Si) or 90.6 MHz (^{13}C). Solutions in CD_2Cl_2 were employed unless otherwise stated. The temperature of the sample was calibrated by means of a standard 10% sample of CH_3OH in CD_3OD whose internal chemical shift has been accurately measured as a function of temperature [34].

Mass spectra were recorded by electron impact. Only the more significant masses are listed; mass values given are for ^{35}Cl and ^{79}Br isotopes.

The ^{13}C NMR spectra of $(\text{Me}_3\text{Si})_3\text{CSiCl}_3$

The methyl region of the ^{13}C NMR spectrum of $(\text{Me}_3\text{Si})_3\text{CSiCl}_3$ comprised a single peak at 276 K at 4.38 ppm, at 216 K signals at 3.60 and 3.47 ppm in an intensity ratio of 1:2, and at 196 K signals at 3.54, 3.40 and 3.34 ppm in an intensity ratio of 1:1:1.

Preparation of $(\text{Me}_3\text{Si})_3\text{CSiBr}_3$

A 1 M solution of Br_2 in benzene (25 ml, 25 mmol) was added dropwise to a stirred solution of $(\text{Me}_3\text{Si})_3\text{CSiH}_3$ [32] (2 g, 7.6 mmol) in benzene (20 ml) cooled to 0°C. The solution was then stirred for a further 1 h during which time the progress of the reaction was monitored by ^1H NMR spectroscopy. The solvent was then removed under reduced pressure to yield a creamy white solid, which was crystallized from CCl_4 to give the new compound (tribromosilyl)tris(trimethylsilyl)methane (3.41 g, 90%). ^1H NMR (CDCl_3 , 296 K) 0.44, (220 K) 0.478 and 0.330 ppm in a ratio 2 : 1, (203 K) 0.466, 0.445 and 0.311 ppm in a ratio 1 : 1 : 1. ^{29}Si NMR (CDCl_3) 0.51 (SiMe_3), -32.31 (SiBr_3). m/z 481 ($[\text{M} - \text{Me}]^+$), 329 ($[\text{M} - \text{Me} - \text{BrSiMe}_3]^+$), 177 ($[\text{M} - \text{Me} - 2 \times \text{BrSiMe}_3]^+$), 73 ($[\text{Me}_3\text{Si}]^+$), 59 ($[\text{Me}_2\text{HSi}]^+$).

Preparation of $(\text{PhMe}_2\text{Si})_3\text{CSiCl}_3$

This compound was prepared in a manner similar to that described [35] for $(\text{PhMe}_2\text{Si})_3\text{CSiMe}_2\text{H}$ by use of the reaction between $(\text{PhMe}_2\text{Si})_3\text{CLi}$ and SiCl_4 , which gave $(\text{PhMe}_2\text{Si})_3\text{CSiCl}_3$ as a white solid, m.p. 195–200°C. ^1H NMR (331 K) 0.82 (s, SiMe_2), 6.9–7.4 (m, SiPh). ^{13}C NMR (306 K) 5.04 (CH_3), 17.01 (CSi_4), 127.85, 129.66, 137.05, 138.44 (aromatic carbons), (216 K) 3.41 and 4.14 (SiMe_2), 14.14 (CSi_4), 127.19, 127.59, 129.10, 135.22, 136.65, 136.97 (aromatic carbons). ^{29}Si NMR 2.28 (SiCl_3) -6.30 (SiMe_2Ph). m/z 550 ($[0.15\% [\text{M}]^+]$), 537 ($0.4 [\text{M} - \text{Me}]^+$), 515 ($0.1 [\text{M} - \text{Cl}]^+$), 499 ($0.2 [\text{M} - \text{HCl} - \text{Me}]^+$), 473 ($0.4 [\text{M} - \text{Ph}]^+$), 463 ($1.2 [\text{M} - 2\text{HCl} - \text{Me}]^+$), 457 ($0.5 [\text{M} - \text{SiMe}_2\text{Cl}]^+$), 197 (21 $[\text{SiMePh}_2]^+$), 135 (100 $[\text{SiMe}_2\text{Ph}]^+$), 93 (10 $[\text{SiMe}_2\text{Cl}]^+$), 73 (15 $[\text{SiMe}_3]^+$).

Determination of the crystal structure of $(\text{PhMe}_2\text{Si})_3\text{CSiCl}_3$

Crystal data: $\text{C}_{25}\text{H}_{33}\text{Cl}_3\text{Si}_4$, $M = 552.2$, space group $P3$, $a = 14.919(5)$, $c = 11.089(4)$ Å, $V = 2137$ Å³, $Z = 3$, $D_c = 1.29$ g cm⁻³, $F(000) = 870$. Monochromated Mo- K_α radiation, $\lambda = 0.71069$ Å, $\mu = 5.01$ cm⁻¹.

A crystal of size $0.85 \times 0.62 \times 1.15$ mm mounted in a glass capillary was used for data collection on an Enraf–Nonius CAD4 diffractometer. Intensities for 8146 reflections with $2 < 2\theta < 50^\circ$ were collected by ω - 2θ scans using a scan width of $0.9 + 0.35 \tan \theta^\circ$. Of these reflections, 2001 were considered observed and unique ($R_{\text{merg}} = 0.086$; $I > 3\sigma(I)$) and were corrected for Lorentz and polarization effects as well as absorption (max/min correction 1.4/0.99).

The structure was solved by routine direct and Fourier methods in the triclinic space group $P1$, after which the atomic positions were transformed and merged such that they fulfilled the requirements of the trigonal space group $P3$. Refinement was effected through blocked-matrix least squares methods, anisotropic thermal parameters being assigned to all non-hydrogen atoms (except the central carbons). A 50:50 disorder present in one of the molecules was treated in the usual fashion. The hydrogens were generated geometrically and were not refined. A Chebyshev weighting scheme with coefficients 48.85, -29.66 and 38.67 gave satisfactory agreement analyses. Refinement converged at $R = 0.104$, $R' = 0.116$.

The structure solution and refinement were carried out using CRYSTALS [36]. Scattering factors for neutral atoms were taken from ref. 37. Final atom coordinates are listed in Table 2 and bond lengths and angles in Table 3. Lists of anisotropic thermal parameters and structure factors are available from P.D.L.

Table 2

Atomic coordinates with estimated standard deviations in parentheses ^a

Atom	x	y	z
Si(1)	0	0	6672(6)
Si(2)	761(4)	1433(5)	8846(5)
Si(2)'	1172(5)	1389(6)	8870(6)
Si(3)	6667	3333	3359(5)
Si(4)	5255(2)	2357(2)	5520(3)
Si(5)	3333	6667	23(5)
Si(6)	3880(3)	5766(3)	2190(4)
Cl(1)	1170(6)	-121(5)	5904(5)
Cl(1)'	1365(7)	1087(8)	5912(9)
Cl(2)	6581(4)	2053(3)	2566(4)
Cl(3)	2234(3)	5328(3)	-768(4)
C(1)	0	0	8401(16)
C(2)	2093(16)	2145(20)	8738(22)
C(3)	288(29)	2224(19)	7792(27)
C(4)	296(19)	1612(24)	10424(24)
C(5)	985(11)	1506(12)	11416(12)
C(6)	481(22)	1677(24)	12459(27)
C(7)	-253(26)	1964(27)	12719(28)
C(8)	-744(26)	2023(29)	11817(26)
C(9)	-393(19)	1975(17)	10629(21)
C(2)'	806(25)	2380(24)	8764(25)
C(3)'	2334(17)	1983(18)	8017(21)
C(4)'	1578(15)	1404(15)	10434(18)
C(6)'	1434(23)	1586(18)	12608(22)
C(7)'	2315(18)	1610(19)	12833(22)
C(8)'	2801(16)	1600(26)	11917(22)
C(9)'	2539(18)	1493(18)	10672(23)
C(10)	6667	3333	5009(15)
C(11)	4340(10)	2839(13)	5491(13)
C(12)	4656(14)	1176(12)	4519(14)
C(13)	5138(8)	1838(9)	7111(10)
C(14)	5141(8)	2406(9)	8160(11)
C(15)	5073(12)	1980(14)	9273(13)
C(16)	4880(15)	1057(14)	9452(14)
C(17)	4821(18)	433(17)	8442(19)
C(18)	4976(15)	858(12)	7304(15)
C(19)	3333	6667	1656(18)
C(20)	5291(11)	6412(15)	2130(13)
C(21)	3451(15)	4596(11)	1204(13)
C(22)	3550(10)	5259(9)	3757(12)
C(23)	4056(11)	5896(11)	4741(12)
C(24)	3873(14)	5519(13)	5943(12)
C(25)	3038(18)	4465(18)	6089(17)
C(26)	2490(19)	3854(12)	5103(17)
C(27)	2770(14)	4232(12)	3979(15)

^a Molecule 1, first orientation comprises Si(1), Si(2), Cl(1) and C(1) to C(9); molecule 1, 2nd orientation comprises Si(1), Si(2)', Cl(1)', C(1), C(5) and C(2)' to C(9)'; molecule 2 comprises Si(3), Si(4), Cl(2) and C(10) to C(18); molecule 3 comprises Si(5), Si(6), Cl(3) and C(19) to C(27).

There are three independent molecules in the unit cell, each of which lies upon a crystallographic three-fold axis (molecule 1 is composed of three asymmetric units such that $x, y, z > -y, x - y, z$ and $> y - x, -x, z$; molecule 2 is composed

Table 3

Intramolecular distances (Å) and angles (°) with estimated standard deviations in parentheses

Molecule 1: 1st orientation

Si(1)–Cl(1)	2.030(7)	Si(1)–C(1)	1.92(2)
Si(2)–C(1)	1.917(5)	Si(2)–C(2)	1.73(2)
Si(2)–C(3)	2.02(3)	Si(2)–C(4)	1.95(2)
C(4)–C(5)	1.57(4)	C(4)–C(9)	1.40(4)
C(5)–C(6)	1.47(3)	C(6)–C(7)	1.39(4)
C(7)–C(8)	1.27(5)	C(8)–C(9)	1.43(4)

Molecule 1: 2nd orientation

Si(1)–Cl(1)'	2.046(9)	Si(1)–C(1)	1.92(2)
Si(2)'–C(1)	2.000(8)	Si(2)'–C(2)'	1.82(4)
Si(2)'–C(3)'	1.77(2)	Si(2)'–C(4)'	1.83(2)
C(4)'–C(5)	1.46(3)	C(4)'–C(9)'	1.40(3)
C(5)–C(6)'	1.46(3)	C(6)'–C(7)'	1.32(4)
C(7)'–C(8)'	1.25(2)	C(8)'–C(9)'	1.42(4)

Molecule 2

Si(3)–Cl(2)	2.048(4)	Si(3)–C(10)	1.83(2)
Si(4)–C(10)	1.952(6)	Si(4)–C(11)	1.83(1)
Si(4)–C(12)	1.89(1)	Si(4)–C(13)	1.90(1)
C(13)–C(14)	1.44(2)	C(13)–C(18)	1.37(2)
C(14)–C(15)	1.37(2)	C(15)–C(16)	1.27(3)
C(16)–C(17)	1.43(3)	C(17)–C(18)	1.38(2)

Molecule 3

Si(5)–Cl(3)	2.043(4)	Si(5)–C(19)	1.81(2)
Si(6)–C(19)	1.979(7)	Si(6)–C(20)	1.83(1)
Si(6)–C(21)	1.88(1)	Si(6)–C(22)	1.86(1)
C(22)–C(23)	1.40(2)	C(22)–C(27)	1.41(2)
C(23)–C(24)	1.42(2)	C(24)–C(25)	1.45(3)
C(25)–C(26)	1.40(3)	C(26)–C(27)	1.35(2)

Molecule 1: 1st orientation

Cl(1)–Si(1)–Cl(1)	103.6(3)	Cl(1)–Si(1)–C(1)	114.8(2)
Si(1)–C(1)–Si(2)	104.9(5)	Si(2)–C(1)–Si(2)	113.6(4)
C(1)–Si(2)–C(2)	121.7(8)	C(1)–Si(2)–C(3)	108.5(8)
C(1)–Si(2)–C(4)	109.3(10)	C(2)–Si(2)–C(3)	103.4(12)
C(2)–Si(2)–C(4)	110.9(11)	C(3)–Si(2)–C(4)	100.8(16)
Si(2)–C(4)–C(5)	108.7(17)	Si(2)–C(4)–C(9)	125.4(23)
C(5)–C(4)–C(9)	124.8(21)	C(4)–C(5)–C(6)	96.7(18)
C(5)–C(6)–C(7)	140.0(30)	C(6)–C(7)–C(8)	115.4(28)
C(7)–C(8)–C(9)	118.9(23)	C(4)–C(9)–C(8)	121.7(23)

Molecule 1: 2nd orientation

Cl(1)'–Si(1)–Cl(1)'	104.2(4)	Cl(1)'–Si(1)–C(1)	114.4(3)
Si(1)–C(1)–Si(2)'	105.1(5)	Si(2)'–C(1)–Si(2)'	113.5(4)
C(1)–Si(2)'–C(2)'	111.3(11)	C(1)–Si(2)'–C(3)'	120.6(11)
C(1)–Si(2)'–C(4)'	111.7(8)	C(2)'–Si(2)'–C(3)'	100.1(11)
C(2)'–Si(2)'–C(4)'	106.5(12)	C(3)'–Si(2)'–C(4)'	105.3(11)
Si(2)'–C(4)'–C(5)	119.6(14)	Si(2)'–C(4)'–C(9)'	119.8(18)
C(5)–C(4)'–C(9)'	119.7(19)	C(4)'–C(5)–C(6)'	114.0(17)
C(5)–C(6)'–C(7)'	125.7(22)	C(6)'–C(7)'–C(8)'	114.9(24)
C(7)'–C(8)'–C(9)'	131.3(25)	C(4)'–C(9)'–C(8)'	113.9(22)

Table 3 (continued)

<i>Molecule 2</i>			
Cl(2)–Si(3)–Cl(2)	102.9(2)	Cl(2)–Si(3)–C(10)	115.4(2)
Si(3)–C(10)–Si(4)	106.9(5)	Si(4)–C(10)–Si(4)	111.9(4)
C(10)–Si(4)–C(11)	116.1(5)	C(10)–Si(4)–C(12)	110.8(7)
C(10)–Si(4)–C(13)	114.7(6)	C(11)–Si(4)–C(12)	105.0(8)
C(11)–Si(4)–C(13)	104.0(6)	C(12)–Si(4)–C(13)	105.1(6)
Si(3)–C(13)–C(14)	122.5(9)	Si(4)–C(13)–C(18)	120.7(10)
C(14)–C(13)–C(18)	116.7(11)	C(13)–C(14)–C(15)	118.6(13)
C(14)–C(15)–C(16)	124.5(15)	C(15)–C(16)–C(17)	119.2(15)
C(16)–C(17)–C(18)	118.4(19)	C(13)–C(18)–C(17)	122.1(18)
<i>Molecule 3</i>			
Cl(3)–Si(5)–Cl(3)	102.9(2)	Cl(3)–Si(5)–C(19)	115.4(2)
Si(5)–C(19)–Si(6)	107.4(6)	Si(6)–C(19)–Si(6)	111.5(5)
C(19)–Si(6)–C(20)	112.9(6)	C(19)–Si(6)–C(21)	113.1(7)
C(19)–Si(6)–C(22)	116.1(7)	C(20)–Si(6)–C(21)	103.6(8)
C(20)–Si(6)–C(22)	104.5(6)	C(21)–Si(6)–C(22)	105.5(6)
Si(5)–C(22)–C(23)	120.6(10)	Si(6)–C(22)–C(27)	120.9(11)
C(23)–C(22)–C(27)	118.5(13)	C(22)–C(23)–C(24)	122.2(13)
C(23)–C(24)–C(25)	115.3(15)	C(24)–C(25)–C(26)	121.8(15)
C(25)–C(26)–C(27)	119.6(17)	C(22)–C(27)–C(26)	122.2(16)

of the three x , y , z , $1 - y$, $x - y$, z and $1 + y - x$, $1 - x$, z ; molecule 3 is composed of the three x , y , z , $1 - y$, $1 + x - y$, z and $y - x$, $1 - x$, z). Two of these (molecules 2 and 3) are enantiomers whilst molecule 1 is a composite of the two conformations disordered in a ratio of 1:1. The possibility of a crystallographic mirror plane running through the latter which transforms one of the former on to the other was explored and rejected. (Topological considerations also lead to this conclusion.)

Acknowledgements

We thank Professor C. Eaborn for helpful discussions and for supplying unpublished X-ray crystal data for $(\text{PhMe}_2\text{Si})_3\text{CSiMe}_2\text{OH}$ and $(\text{PhMe}_2\text{Si})_3\text{CSiMeH}(\text{OH})$, and Mr S.M. Whittaker for experimental assistance.

References

- 1 See, for example, C. Eaborn, in H. Sakurai (Ed.), *Organosilicon and Bioorganosilicon Chemistry*, Ellis Horwood, Chichester, 1985, pp. 123–130; J.D. Smith, *Pure Appl. Chem.*, 58 (1986) 623 and refs. therein.
- 2 C. Eaborn, P.B. Hitchcock, P.D. Lickiss and K.D. Safa, *J. Chem. Soc., Dalton Trans.*, (1984) 2015.
- 3 A.G. Avent, P.D. Lickiss and A. Pidcock, *J. Organomet. Chem.*, 341 (1988) 281.
- 4 H.M. McConnell, *J. Chem. Phys.*, 28 (1958) 430.
- 5 Nottingham Algorithm Group Computer Applications Library.
- 6 J.H. Wilkinson and C. Reinsch, *Handbook of Automatic Computation, Volume II, Linear Algebra*, Springer-Verlag, Berlin, 1971, pp. 93–110.
- 7 W.D. Hounshell, L.D. Iroff, R.J. Wroczynski and K. Mislow, *J. Am. Chem. Soc.*, 100 (1978) 5212.
- 8 M. Weidenbruch, W. Peter and C. Pierrard, *Angew. Chem., Int. Ed. Engl.*, 15 (1976) 43.
- 9 M. Weidenbruch, H. Flott, J. Fleischhauer and W. Schleker, *Chem. Ber.*, 115 (1982) 3444.
- 10 Taken from footnote 19 in ref. 12.

- 11 R.J. Wroczynski, L.D. Iroff and K. Mislow, *J. Org. Chem.*, 43 (1978) 4236.
- 12 R.J. Wroczynski and K. Mislow, *J. Am. Chem. Soc.*, 110 (1979) 3980.
- 13 D.G. Anderson, D.W.H. Rankin, H.E. Robertson, A.H. Cowley and M. Pakulski, *J. Mol. Struct.*, 196 (1989) 21.
- 14 A.H. Cowley, J.E. Kilduff, E.A.V. Ebsworth, D.W.H. Rankin, H.E. Robertson and R. Seip, *J. Chem. Soc., Dalton Trans.*, (1984) 689.
- 15 B. Beagley, R.G. Pritchard and J.O. Titiloye, *J. Mol. Struct.*, 212 (1988) 323.
- 16 L.S. Bartell, F.B. Clippard Jr. and T.L. Boates, *Inorg. Chem.*, 9 (1970) 2436.
- 17 L.D. Iroff and K. Mislow, *J. Am. Chem. Soc.*, 100 (1978) 2121.
- 18 N.H. Buttrus, C. Eaborn, M.N.A. El-Kheli, P.B. Hitchcock, J.D. Smith, A.C. Sullivan and K. Tavakkoli, *J. Chem. Soc., Dalton Trans.*, (1988) 381.
- 19 C. Eaborn, P.B. Hitchcock, P.D. Lickiss and A.D. Taylor, *J. Organomet. Chem.*, 398 (1990) 59.
- 20 C. Eaborn, P.B. Hitchcock and P.D. Lickiss, *J. Organomet. Chem.*, 269 (1984) 235.
- 21 J.L. Atwood, S.G. Bott, P.B. Hitchcock, C. Eaborn, R.S. Shariffudin, J.D. Smith and A.C. Sullivan, *J. Chem. Soc., Dalton Trans.*, (1987) 747.
- 22 S.S. Al-Juaid, N.H. Buttrus, C. Eaborn, P.B. Hitchcock, J.D. Smith and K. Tavakkoli, *J. Chem. Soc., Chem. Commun.*, (1988).
- 23 J.L. Atwood, S.G. Bott, C. Eaborn, M.N.A. El-Kheli and J.D. Smith, *J. Organomet. Chem.*, 294 (1985) 23.
- 24 C. Eaborn, M.N.A. El-Kheli, P.B. Hitchcock and J.D. Smith, *J. Chem. Soc., Chem. Commun.*, (1984) 1673.
- 25 S.S. Al-Juaid, S.M. Dhaher, C. Eaborn, P.B. Hitchcock and J.D. Smith, *J. Organomet. Chem.*, 325 (1987) 117.
- 26 S.S. Al-Juaid, S.M. Dhaher, C. Eaborn, P.B. Hitchcock, C.A. McGeary and J.D. Smith, *J. Organomet. Chem.*, 366 (1989) 39.
- 27 A. Alvanipour, N.H. Buttrus, C. Eaborn, P.B. Hitchcock, A.I. Mansour and A.K. Saxena, *J. Organomet. Chem.*, 349 (1988) 29.
- 28 S.S. Al-Juaid, N.H. Buttrus, C. Eaborn, P.B. Hitchcock, A.T.L. Roberts, J.D. Smith and A.C. Sullivan, *J. Chem. Soc., Chem. Commun.*, (1986) 908.
- 29 S.S. Al-Juaid, A.K.A. Al-Nasr, C. Eaborn and P.B. Hitchcock, *J. Chem. Soc., Chem. Commun.*, (1991) 1482.
- 30 C. Eaborn, personal communication.
- 31 C. Eaborn, M.N.A. El-Kheli, P.B. Hitchcock and J.D. Smith, *J. Organomet. Chem.*, 272 (1984) 1.
- 32 S.S. Dua, C. Eaborn, D.A.R. Happer, S.P. Hopper, K.D. Safa and D.R.M. Walton, *J. Organomet. Chem.*, 178 (1979) 75.
- 33 S.S. Al-Juaid, S.M. Dhaher, C. Eaborn, P.B. Hitchcock, C.A. McGeary and J.D. Smith, *J. Organomet. Chem.*, 366 (1989) 39.
- 34 A.L. van Geet, *Anal. Chem.*, 42 (1970) 679.
- 35 C. Eaborn and A.I. Mansour, *J. Chem. Soc., Perkin Trans. 2*, (1985) 729.
- 36 D.J. Watkin, J.R. Carruthers and P.W. Betteridge, *CRYSTALS User Manual*, Chemical Crystallography Laboratory, University of Oxford, 1985.
- 37 *International Tables of Crystallography*, Kynoch Press, Birmingham, UK, 1974.
- 38 A.G. Avent and P.D. Lickiss, unpublished results.